WATER RESOURCES RESEARCH, VOL. 35, NO. 10, PAGES 2965–2979, OCTOBER 1999

Estimating unsaturated soil hydraulic properties from laboratory tension disc infiltrometer experiments

Jiří Šimůnek

U. S. Salinity Laboratory, USDA-ARS, Riverside, California

Ole Wendroth

Institute for Soil Landscape Research, Zentrum für Agrarlandschafts und Landnutzungsforschung Müncheberg, Germany

Martinus T. van Genuchten

U. S. Salinity Laboratory, USDA-ARS, Riverside, California

Abstract. Four tension disc infiltration experiments were carried out on a loamy soil in the laboratory for the purpose of estimating the unsaturated soil hydraulic properties. Sixteen tensiometers were installed in pairs at the following coordinate (r, z) positions: (10, 2.5), (10, 5), (10, 10), (15, 5), (15, 10), (15, 15), (15, 20), and (15, 30), where r represents the distance from the axis of symmetry and z is the location below the soil surface. A time domain reflectometry (TDR) probe was used to measure water contents at a depth of 2 cm directly below the tension disc. The first three experiments involved supply pressure heads at the disc of -20, -10, -5, and -1 cm, with the experiment lasting for ~5 hours. The same supply pressure heads were also used for the fourth experiment, which lasted 6.25 days so as to reach steady state at each applied tension. The measured data were analyzed using *Wooding*'s [1968] analytical solution and by numerical inversion. The parameter estimation method combined a quasi three-dimensional numerical solution of the Richards equation with the Marquardt-Levenberg optimization scheme. The objective function for the parameter estimation analysis was defined using different combinations of the cumulative infiltrated volume, TDR readings, and tensiometer measurements. The estimated hydraulic properties were compared against results obtained with an evaporation experiment as analyzed with *Wind*'s [1968] method. Water contents in the retention curves were underestimated when both transient and quasi steady state experiments were analyzed by parameter estimation. Unsaturated hydraulic conductivities obtained by parameter estimation and using *Wooding*'s [1968] analysis corresponded well. Drying branches of the hydraulic conductivity function determined by parameter estimation also corresponded well with those obtained with the evaporation method.

1. Introduction

More attention is increasingly being directed to accurate measurement of the unsaturated soil hydraulic properties close to saturation [*van Genuchten et al*., 1999], i.e., to moisture conditions that are strongly affected by soil structure and macropores. Traditional transient laboratory methods, such as outflow or evaporation experiments, show relatively little sensitivity to the hydraulic conductivity at near-saturated conditions and hence are more suitable for estimating the hydraulic conductivity at medium saturation levels. The evaporation method usually fails in the near-saturation range where the hydraulic conductivity is highest, leading to very small hydraulic gradients that cannot be determined with sufficient accuracy [*Wendroth and Šimůnek*, 1999]. Hence there is a trend toward determining the hydraulic conductivity in the wet range with steady state experiments, such as the tension disc infiltrometer method [*Perroux and White*, 1988] or the crust method [*Bouma et al*., 1971], whereas transient conditions are used for the drier range [*Wendroth and Šimůnek*, 1999].

Tension disc infiltrometers have recently become very popular devices for in situ measurement of the near-saturated soil hydraulic properties [*Perroux and White*, 1988; *Ankeny et al*., 1991; *Reynolds and Elrick*, 1991; *Logsdon et al*., 1993]. Thus far, tension infiltration data have been used primarily for evaluating saturated and unsaturated hydraulic conductivities and for quantifying the effects of macropores and preferential flow paths on infiltration. Tension infiltration data are generally used to evaluate the saturated hydraulic conductivity K_s and the sorptive number α^* given by *Gardner*'s [1958] exponential model (equation (10) below) of the unsaturated hydraulic conductivity using *Wooding*'s [1968] analytical solution. Analyses of this type require either two infiltration measurements using two different disc diameters [*Smettem and Clothier*, 1989] or measurements using a single disc diameter but with multiple tensions [e.g., *Ankeny et al*., 1991].

Detailed studies of the water flow field below the tension disc infiltrometer have been limited. In most studies the final water content and/or concentration profiles were obtained by

Paper number 1999WR900179.

sampling after terminating the infiltration experiment [e.g., *Clothier et al*., 1992; *Quadri et al*., 1994]. *Clothier et al*. [1992] used knowledge of the steady state water and solute (Br^-) distributions to estimate the mobile and immobile water fractions. *Quadri et al*. [1994] used a similar experimental setup to validate their finite difference numerical model for axisymmetrical movement of both water and solute underneath a quarter-sector disc permeameter. They obtained good predictions for the observed moisture and Br^- profiles in the sandbox as well as for the measured infiltration rate from the disc [*Quadri et al*., 1994].

Recent developments in TDR technology have provided vadose zone hydrologists and soil scientists with a tool for quick and accurate measurement of the water content and the bulk electric conductivity. *Kachanoski et al*. [1990] used both straight and curved TDR transmission lines to measure soil water distributions as a function of time at different radial distances from the surface water source during three-dimensional infiltration in a laboratory setup. A similar setup was used by *Ward et al*. [1994] to characterize both water flow and solute transport underneath a disc infiltrometer. Recently, *Vogeler et al*. [1996] used horizontally and vertically installed TDR probes to characterize simultaneously water and solute movement below a disc permeameter in a one-dimensional setup and successfully modeled measured data with a numerical model. The above studies were all carried out in the laboratory. In contrast, *Wang et al*. [1998] measured water contents with TDRs and pressure heads with tensiometers in a field experiment to develop and test different approximate analytical infiltration models in their inverse analysis.

Although early time infiltration data can be used to estimate the sorptivity [*White and Sully*, 1987] and, consequently, the matrix flux potential, only steady state infiltration rates are usually used for Wooding-type analyses. We recently suggested using the entire cumulative infiltration curve in combination with parameter estimation to estimate additional soil hydraulic parameters [*Šimůnek and van Genuchten*, 1996, 1997]. From an analysis of numerically generated data for one supply tension experiment we concluded that the cumulative infiltration curve by itself does not contain enough information to provide a unique inverse solution [*Šimůnek and van Genuchten*, 1996]. An infinite number of combinations of the saturated hydraulic conductivity, K_s and the shape factor n (see (6) and (7)) can result in almost identical infiltration curves. A similar conclusion was reached by *Russo et al*. [1991] for a one-dimensional ponded infiltration experiment. Hence additional information about the flow process, such as the water content and/or pressure head, measured at one or more locations in the soil profile is needed to successfully obtain unique inverse solutions for the soil hydraulic functions.

Šimůnek and van Genuchten [1997] studied, again numerically, infiltration at several consecutive supply tensions. Šimůnek and van Genuchten considered several different scenarios with different levels of information and concluded that the best practical scenario is to estimate the hydraulic parameters from the cumulative infiltration curve measured at several consecutive tensions applied to the soil surface, in conjunction with knowledge of the initial and final water content. Our results suggested that one should be able to use information typically being collected with a tension disc infiltrometer to estimate not only unsaturated hydraulic conductivities but also, without further experiments, the soil water retention properties.

The above methodology was tested on data collected as part of the soil hydrology program of the Hydrologic Atmospheric Pilot Experiment (HAPEX)-Sahel regional-scale experiment [*Cuenca et al*., 1997]. *Šimůnek et al*. [1998a] showed that it is indeed possible to obtain relatively reliable estimates of soil hydraulic conductivities for near-saturated moisture conditions from tension disc infiltration data by numerical inversion, consistent with results of the traditional Wooding analysis. However, the question of whether it is possible also to estimate simultaneously the retention curve was not resolved satisfactorily.

Infiltration rates effectively integrate properties of the porous media underneath the disc infiltrometer, including the influence of local-scale heterogeneity, different soil structure, and texture irregularities, preferential pathways, layering, and anisotropy; hence infiltration rates provide a good way for estimating the effective near-saturated soil hydraulic properties. The question of whether a more detailed description of the flow field, for example, in terms of point measurements of the pressure head and water content at several locations of the soil profile, can improve the parameter estimation process and lead to more precise estimates of the effective soil hydraulic properties arises. Our previous studies also did not resolve several other questions concerning the best definition of the objective function, such as (1) how the objective function should be defined and which measurements should be included; (2) what the importance is of different types of data and what these can do to improve the parameterization of soil hydraulic properties; (3) whether or not one should include all available measurements in the definition of the objective function, such as pressure head measurements, water content measurements, or cumulative infiltration volumes, or only some (and which) optimal combination of these; (4) if and how a combination of different sets of measurements can augment each other and what weight should be given to particular measurement sets so that one measurement set does not dominate the others; and finally, (5) whether the weighting should be closely related to expected data errors or should reflect the expected importance of a particular measurement set to the parameterization of the soil hydraulic properties.

In this study we will apply the parameter estimation technique to the analysis of tension disc infiltrometer laboratory experiments in which the soil profile is instrumented with both time domain reflectometry (TDR) (at one location) and tensiometers (at several locations) to measure water contents and pressure heads with time. The soil hydraulic characteristics estimated using different sets of information will be compared against results of *Wooding*'s [1968] analysis and against independently measured soil hydraulic properties obtained with the evaporation method.

2. Experiment

The experiments were carried out using a loamy sand soil that was sieved through a 4 mm mesh sieve. The soil was carefully repacked in a $1 \times 1 \times 1$ m^3 soil container in 10 cm layers at an initial soil bulk density of 1.5 g cm^{-3}. After packing in the laboratory the soil container was taken outside and exposed to natural rainfall and evaporation conditions for ~2.5 years. During this time all germinated weeds were removed by hand. In December 1996 the soil container was brought back into the laboratory, the upper 10 cm soil layer was removed, and the soil was carefully leveled. Pressure transducer tensiometers (measurement errors ±0.5 cm) were installed horizontally at different depths and at different distances relative

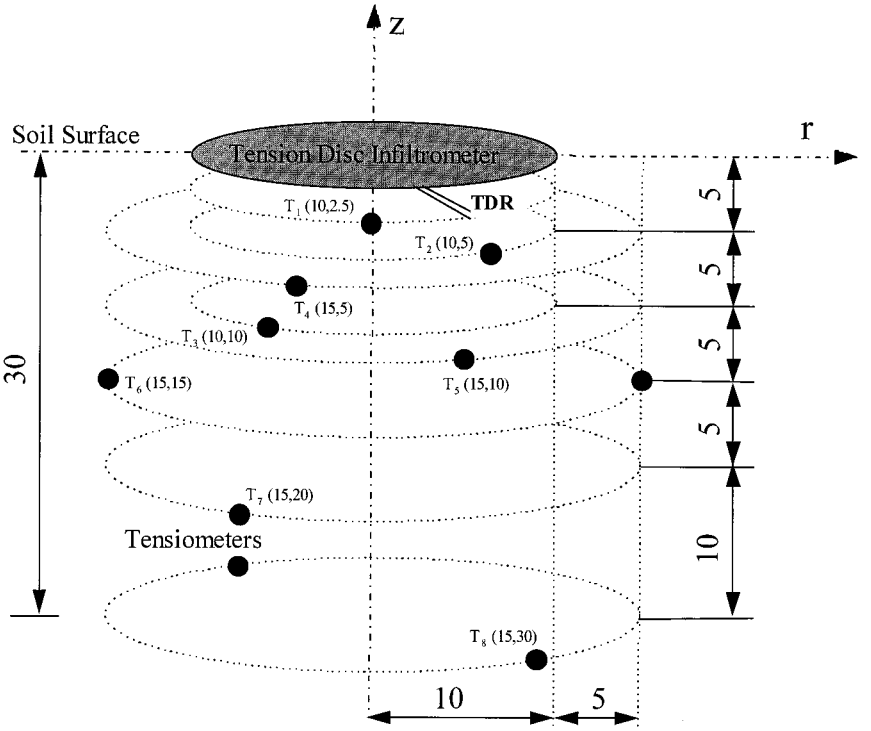

Figure 1. Schematic of tension disc infiltrometer setup, including time domain reflectometry (TDR) probe and tensiometers T_1 through T_8.

to the center of the permeameter (Figure 1). A small hole for this purpose was hand dug to the intended measurement depth and then used for inserting tensiometer from the side. The hole was far enough from the central vertical axis below the disc to avoid soil disturbance within the flow domain. After installation the holes were filled with soil. The tensiometer cups of 6 cm length and 0.6 cm outside diameter were isolated, with the exception of their 1 cm long tips. Sixteen tensiometers were installed in pairs at the following coordinate (r, z) positions: (10, 2.5), (10, 5), (10, 10), (15, 5), (15, 10), (15, 15), (15, 20), and (15, 30), where r represents the distance from the axis of symmetry and z is the location below the soil surface. A two-wire TDR probe (measurement error ± 0.01 m^3 m^{-3}) was horizontally installed at a depth of $\sim$2 cm directly below the tension disc. The TDR rods were 10 cm long and $\sim$1.5 cm apart. Prior to the disc infiltration experiment a plexiglass ring of 2 cm height was inserted in the soil to a depth of $\sim$1.5 cm. In order to avoid smearing of the soil surface and closing pores by surface smoothing a fine sand layer was placed on the soil surface within the ring to ensure good contact between the tension disc and the soil. In our device the tension disc was connected via a PVC pipe to a water reservoir placed at the intended height relative to the soil surface in the container. The tension disc was subsequently put on the soil surface, and the water supply was opened. The infiltrometer disc had a radius of 10 cm. A schematic of the locations of the tensiometers, the TDR probe, and the infiltrometer disc is shown in Figure 1.

We conducted four infiltration experiments, each with consecutively increasing supply pressure heads of -20, -10, -5, and -1 cm. The first three experiments lasted between 4.5 and 5.5 hours and are referred to here as the "short" or "unsteady state" experiments. The supply tension of -1 cm was applied for $\sim$25 min, and the pressure heads of -5 and -10 cm were applied for $\sim$65 min. The last experiment lasted 6.25 days and will be referred to it as the "long" or "steady state" experiment. The first tension in this fourth experiment was applied for nearly 4 days, the second tension was applied for $\sim$2 days, and the last two tensions were applied for 6 and 1 hour, respectively. The intent of the fourth experiment was to reach steady state at each applied tension so that *Wooding*'s [1968] analytical solution could be used. Tensiometer readings were taken automatically every 30 s. We monitored the water level in the infiltrometer, as well as the TDR, about every 5 minutes, except for the -1 cm supply head where readings were obtained every minute. Since the infiltration tubes did hold only $\sim$2 L of water, the experiments had to be interrupted several times during refilling. In order to capture also the redistribution part of the experiment, tensiometers were read for an additional 2 hours after infiltration had ceased. A summary of the experimental conditions is given in Table 1. Between experiments the water in the soil container was allowed freely to redistribute and evaporate through the unprotected soil surface to recreate approximately similar initial conditions.

Ten undisturbed soil core samples with a height of 6 cm and an inside diameter of 8 cm were used independently to measure the soil hydraulic properties. From the 10 samples, five were taken at 2–8 cm depth, and the five at 10–16 cm depth were taken at a distance of at least 50 cm away from the infiltration disc. The average bulk density of the samples was 1.41 g cm^{-3}. Unsaturated soil hydraulic conductivities close to saturation (at pressure heads of -1, -5, and -10 cm) were determined using steady state downward infiltration experiments with two tension disc permeameters [*Wendroth and Šimůnek*, 1999]. One infiltrometer disc was placed at the top and another one at the bottom of the soil sample. The same

Table 1. Summary of Experimental Conditions for the Four Tension Disc Infiltration Experiments

Experiment	Supply Tensions	Experiment Duration			Infiltrated Volume, L	Initial Pressure Heads, cm		Final Infiltration Rates, $cm^3\ s^{-1}$
		Days	Hours	Minutes		2.5 cm Depth	30 cm Depth	
I	20 cm		2	39	0.084			0.00330
	10 cm		1	10	0.522			0.0767
	5 cm		1	5	1.213	−493	−200	0.379
	1 cm			24	4.304			3.81
	Total		5	18	6.12			
II	20 cm		2	7	0.155			0.0154
	10 cm		1	6	0.647			0.122
	5 cm		1	6	1.502	−498	−210	0.436
	1 cm			20	4.224			2.67
	Total		4	39	6.53			
III	20 cm		2	3	0.213			0.0291
	10 cm		1	5	0.470			0.0984
	5 cm		1	6	1.549	−336	−182	0.442
	1 cm			25	4.465			3.86
	Total		4	39	6.70			
IV	20 cm	3	23		5.92			0.0143
	10 cm	2		15	10.12			0.0586
	5 cm		5	48	4.15	−641	−222	0.224
	1 cm		1	2	14.33			4.04
	Total	6	6	5	34.5			

pressure head was applied to both discs in order to establish and maintain steady state flow conditions under a unit gradient and from this to obtain unsaturated hydraulic conductivities. Following the infiltrometer experiments, the samples were moved onto impermeable plates to determine water retention and unsaturated hydraulic conductivity data for pressure heads <-10 cm using two-rate evaporation experiments [*Wendroth et al*., 1993; *Šimůnek et al*., 1998b]. The resulting data were analyzed using a modified *Wind* [1968] method [*Wendroth et al*., 1993]. After conclusion of the evaporation experiments the water contents at pressure heads of −10 and −150 m were measured in a pressure chamber on selected 0.7 cm long subsamples from the disturbed cores.

3. Theory

3.1. Numerical Model

In our analysis of the tension disc infiltrometer data we will use a numerical solution of the Richards' equation coupled with the Levenberg-Marquardt nonlinear minimization method [*Marquardt*, 1963]. The governing flow equation for radially symmetric isothermal Darcian flow in a variably saturated isotropic rigid porous medium is given by the following modified form of the Richards' equation:

$$\frac{\partial \theta}{\partial t} = \frac{1}{r}\frac{\partial}{\partial r}\left(rK\frac{\partial h}{\partial r}\right) + \frac{\partial}{\partial r}\left(K\frac{\partial h}{\partial z}\right) - \frac{\partial K}{\partial z}, \tag{1}$$

where θ is the volumetric water content $[L^3L^{-3}]$, h is the pressure head $[L]$, K is the hydraulic conductivity $[LT^{-1}]$, r is a radial coordinate $[L]$, z is the vertical coordinate $[L]$ positive downward, and t is time $[T]$. Equation (1) was solved numerically for the following initial and boundary conditions applicable to a disc tension infiltrometer experiment:

$$\theta(r, z, t) = \theta_i(z) \quad t = 0,$$
$$h(r, z, t) = h_i(z) \quad t = 0, \tag{2}$$

$$h(r, z, t) = h_0(t) \quad 0 < r < r_0 \qquad z = 0, \tag{3}$$

$$\frac{\partial h(r, z, t)}{\partial z} = 1 \quad r > r_0 \qquad z = 0, \tag{4}$$

$$h(r, z, t) = h_i \quad r^2 + z^2 \to \infty, \tag{5}$$

where θ_i is the initial water content $[L^3L^{-3}]$, h_i is the initial pressure head $[L]$, h_0 is the time variable supply pressure head imposed by the tension disc infiltrometer $[L]$, and r_0 is the disc radius $[L]$. Equation (2) specifies the initial condition in terms of either the water content or the pressure head. Boundary condition (3) prescribes the time variable pressure head under the tension disc permeameter, while (4) assumes a zero flux at the remainder of the soil surface (evaporation is neglected during the short-duration infiltration experiments). Equation (5) states that the other boundaries are sufficiently distant from the infiltration source so that they do not influence the flow process. The boundary condition at the axis of symmetry ($r = 0$) is a no flow condition. Equation (1), subject to the above initial and boundary conditions, was solved using a quasi three-dimensional (axisymmetric) finite element code, HYDRUS-2D, as documented by *Šimůnek et al*. [1996].

3.2. Soil Hydraulic Properties

A model of the unsaturated soil hydraulic properties must be selected prior to application of the numerical solution of the Richards' equation. In this study we will limit ourselves to the unsaturated soil hydraulic functions [*van Genuchten*, 1980]:

$$S_e(h) = \frac{\theta(h) - \theta_r}{\theta_s - \theta_r} = \frac{1}{(1 + |\alpha h|^n)^m} \tag{6}$$

$$K(\theta) = K_s S_e^l [1 - (1 - S_e^{1/m})^m]^2, \tag{7}$$

where S_e is the effective fluid saturation [ ], K_s is the saturated hydraulic conductivity $[LT^{-1}]$, θ_r and θ_s denote the residual and saturated water contents $[L^3L^{-3}]$, respectively; l is the pore connectivity parameter [ ], and α $[L^{-1}]$, n [ ], and m $(= 1 - 1/n)$ [ ] are empirical shape parameters. The pore connectivity parameter l in $K(\theta)$ was estimated by *Mualem* [1976] to be 0.5 as an average for many soils. Taking

$l = 0.5$, the above hydraulic functions contain five unknown parameters: θ_r, θ_s, α, n, and K_s. We will refer to (6) and (7) as the van Genuchten-Mualem (VGM) model.

3.3. Formulation of the Inverse Problem

The objective function Φ to be minimized during the parameter estimation process can be formulated in terms of an arbitrary combination of cumulative infiltration data, TDR-measured water contents, and/or tensiometer (pressure head) readings. The objective function is defined as [*Šimůnek and van Genuchten*, 1996]

$$\Phi(\boldsymbol{\beta}, \mathbf{q_m}) = \sum_{j=1}^{m} \left\{ v_j \sum_{i=1}^{n_j} w_{ij}[q_j^*(t_i) - q_j(t_i, \boldsymbol{\beta})]^2 \right\}, \quad (8)$$

where m represents different sets of measurements (infiltration data, pressure heads, and/or water contents), n_j is the number of measurements in a particular set, $q_j^*(t_i)$ is the specific measurement at time t_i for the jth measurement set, $\boldsymbol{\beta}$ is the vector of optimized parameters (e.g., θ_r, θ_s, α, n, K_s, and l), $q_j(t_i, \boldsymbol{\beta})$ represents the corresponding model predictions for parameter vector $\boldsymbol{\beta}$, and v_j and w_{ij} are weights associated with a particular measurement set j or a measurement i within set j, respectively. We assume that the weighting coefficients w_{ij} in (8) are equal to 1; that is, the variances of the errors inside a particular measurement set are all the same. The weighting coefficients v_j are given by

$$v_j = \frac{1}{n_j \sigma_j^2}. \quad (9)$$

The above approach views the objective function as the average weighted squared deviation normalized by measurement variances σ_j^2. Minimization of the objective function Φ is accomplished by using the Levenberg-Marquardt nonlinear minimization method [*Marquardt*, 1963].

3.4. *Wooding*'s [1968] Analysis

The traditional analysis of tension disc infiltration data based on *Wooding*'s [1968] analytical solution requires two steady state fluxes at different tensions [*Ankeny et al*., 1991] to yield estimates of the saturated hydraulic conductivity K_s $[LT^{-1}]$ and the sorptive number α^* $[L^{-1}]$ in *Gardner*'s [1958] exponential model of the unsaturated hydraulic conductivity:

$$K(h) = K_s \exp(\alpha^* h), \quad (10)$$

Wooding's solution for infiltration from a circular source with a constant pressure head at the soil surface, and with the unsaturated hydraulic conductivity described by (10), is given by

$$Q(h_0) = \pi r_0^2 K(h_0) + \frac{4r_0}{\alpha^*} K(h_0). \quad (11)$$

where Q is the steady state infiltration rate $[L^3T^{-1}]$, r_0 is the radius of the disc $[L]$, h_0 is the wetting pressure head $[L]$, and $K(h_0)$ is the unsaturated hydraulic conductivity $[LT^{-1}]$ at pressure head h_0. Methods for obtaining the unsaturated hydraulic conductivity in the middle of an interval between two successively applied pressure heads are given by *Ankeny et al*. [1991], *Reynolds and Elrick* [1991], and *Jarvis and Messing* [1995], among others.

Table 2a. Unsaturated Hydraulic Conductivities Calculated Using *Wooding*'s [1968] Analysis

	Unsaturated Hydraulic Conductivity, cm s^{-1}		
Experiment	$h = -15$ cm	$h = -7.5$ cm	$h = -3$ cm
I	0.0000361	0.000388	0.00313
II	0.0000855	0.000489	0.00268
III	0.0000833	0.000466	0.00337
IV	0.0000485	0.000247	0.00257
Arithmetic mean	0.0000634	0.000398	0.00294

4. Results and Discussion

4.1. *Wooding*'s [1968] Analysis

Experimental data were first analyzed using *Wooding*'s [1968] analytical solution (see (11)). Wooding's analysis requires steady state infiltration rates at different supply pressure heads. Depending upon soil texture it can take hours or even days to reach steady state in a field experiment. Previous studies have shown that Wooding's approach will overestimate the soil hydraulic conductivity if steady state infiltration is not reached. Nevertheless, infiltration rates reached within 1 hour are assumed to be the steady state rates in a majority of studies and are used in Wooding's analysis. The possible error is usually dismissed as being negligible as compared to the effects of soil heterogeneity. Another reason for dismissing errors caused by not reaching steady state infiltration is the lack of reproducibility of infiltration experiments. For our soil, differences between the final infiltration rates for the same type of experiments (i.e., the short experiments I–III) were larger than the increased precision resulting from the use of steady state infiltration rates as obtained with the long experiment (experiment IV) at particular supply tensions (Table 1). Actually, the final infiltration rates for the long experiment were sometimes higher than the final infiltration rates for the short experiments. The problems of reproducibility of unsaturated soil flow experiments was also raised by *Císlerová et al*. [1988], who found that steady state ponded infiltration rates in a coarse acid brown soil depended strongly on the initial moisture content. They contributed this effect to entrapped air that alters the volume of available pores for flow. Such an effect of the initial water content on infiltration rate was not evident from our data. *Hollenbeck and Jensen* [1998] studied transient outflow laboratory experiments and also found that experiments with small changes in the imposed boundary conditions could not be reproduced well even when great care was taken to reproduce the same initial conditions. Although experiments with large step changes were reproduced better, the overall system response was virtually the same for all step levels [*Hollenbeck and Jensen*, 1998].

Estimated unsaturated hydraulic conductivities at pressure heads in the middle of the imposed disc supply intervals are presented in Table 2a. As expected, the calculated conductivities, with one exception at $h = -15$ cm, were lowest for the fourth experiment, where steady state infiltration rates were presumably reached at each supply tension. The smallest deviations (of ~15%) between the calculated conductivities and their arithmetic means were for $h = -3$ cm, while the largest deviations, ~75%, occurred for $h = -15$ cm. Overall, the differences between unsaturated hydraulic conductivities calculated using Wooding's analysis at any particular supply pressure head were relatively small. Also, differences between K_s

Table 2b. Saturated Hydraulic Conductivities and Sorptive Numbers α^* Calculated Using *Wooding*'s [1968] Analysis

Experiment	Saturated Hydraulic Conductivity, cm s^{-1}/Sorptive Number, α^* cm^{-1}		
	$h(-20, -10)$	$h(-10, -5)$	$h(-5, -1)$
I	0.00404/0.315	0.00425/0.319	0.0177/0.578
II	0.00191/0.207	0.00330/0.254	0.0104/0.453
III	0.000517/0.122	0.00443/0.300	0.0171/0.542
IV	0.000401/0.141	0.00185/0.268	0.0225/0.723
Arithmetic mean	0.00172/0.196	0.00346/0.285	0.0169/0.574

values extrapolated from the same supply tension intervals for different experiments were relatively small (Table 2b). The smallest differences occurred for those calculated using the largest pressure heads, $h(-5, -1)$, while the largest differences (almost 1 order of magnitude) arose for those using the lowest pressure heads, $h(-20, -10)$. Saturated hydraulic conductivities calculated using the largest supply tension interval were almost 1 order of magnitude lower than those obtained for the smallest tension interval (Table 2b). Similarly, the sorptive number α^* was much lower for the largest interval than for the smallest one. Because the predicted values of α^* for different tension intervals differed substantially, applicability of *Gardner*'s [1958] model for extrapolation of the unsaturated hydraulic conductivity function beyond a particular supply tension interval is questionable, at least for the loamy sand used in our study.

4.2. Numerical Inversions

The measured data were next analyzed using parameter estimation by combining the HYDRUS-2D numerical code [*Šimůnek et al*., 1996] with the Levenberg-Marquardt nonlinear minimization method [*Marquardt*, 1963]. The computational domains (r, z) for the numerical solution of either 50×50 cm^2 or 100×100 cm^2 were discretized into structured rectangular finite element mesh grids containing 15×19 and 24×33 mesh nodes for the first three experiments and the last experiment, respectively. A finer discretization was used near the soil surface than at depth. A much larger transport area for the fourth experiment was used because of the longer duration of the experiment and the larger cumulative infiltrated volume.

As the initial condition, we used the arithmetic mean of the pressure head for all functioning tensiometers at a particular depth (maximum 4) and linear interpolation between the averaged pressure heads at those depths. In one special case we assumed that the initial condition was constant for the entire soil profile and equal to the measured initial water content at a depth of 2 cm. The assumption of homogeneity in the initial condition likely would introduce some error in the calculations since the initial condition was not constant (see Table 1). The initial water content in the immediate vicinity of the tension disc, together with the supply tension, defines the soil sorptivity and the curvature of the cumulative infiltration curve. This curvature is generally highest at the beginning of infiltration experiment when the capillary forces are dominating the infiltration process. The initial condition farther away from the infiltrometer disc has far less effect on the shape of the cumulative infiltration curve; it affects primarily the speed of the infiltration front through the soil profile. Our ultimate objective here was to estimate the soil hydraulic parameters from the least amount of information possible. Although a somewhat incorrect or incomplete description of the initial condition may not yield accurate descriptions of the flow field in the soil, errors in terms of the calculated cumulative infiltration curve may only be minimal.

The measured data were analyzed in several different ways. We first used four different formulations for the objective function. Cumulative infiltration volumes $I(t)$, which represent an integral characteristic of the soil profile, were included in the definition of the objective function for all optimizations. We additionally used either all other measured data simultaneously or combined the cumulative infiltration volumes with either only the pressure head or water content data. In one case we defined the objective function in terms of the measured cumulative infiltration and the final water content as measured with the TDR at 2 cm depth. This measured final water content θ_f was assumed to define one point of the retention curve together with the final supply pressure head (-1 cm). This optimization option, in combination with the initial condition being defined in terms of the water content, represents the optimization scenario that was suggested by *Šimůnek and van Genuchten* [1997] as being the best practical setup for predicting the soil hydraulic parameters from a tension infiltration experiment.

Next we optimized the soil hydraulic parameters in the VGM model with and without assuming hysteresis according to *Kool and Parker* [1987] (referred to here as the VGM-H model). In a final scenario we also optimized the pore connectivity number l (VGM-Hl model). Below we will concentrate mainly on experiment III, representing the short experiments, and steady state experiment IV. The soil hydraulic parameters obtained with different optimization options for experiments III and IV are summarized in Tables 3 and 4, respectively. In our analysis we used 44 water content, 22,752 pressure head, and 62 cumulative infiltration data points for experiment III and 91 water content, 12,564 pressure head, and 100 cumulative infiltration data points for experiment IV.

4.2.1. Experiment III. Selected results for different parameter optimization options for experiment III (the short-duration infiltration experiment that lasted ~4.5 hours) are summarized in Table 3. In this table, Φ_I^*, Φ_h^*, and Φ_θ^* represent contributions to the total value of the objective function Φ of the weighted residuals between measured and optimized values of the cumulative infiltration, pressure head, and water content measurement sets, respectively. Symbols in front of a semicolon within the argument of Φ (Table 3) represent measurement sets used in the optimization, while parameters listed after the semicolon define the optimized unknowns. The best fit for any particular measurement set (i.e., cumulative infiltration, water content, or pressure heads data) and the best overall fit as characterized by the highest R^2 and the lowest value of the objective function Φ are shown. For comparison the last column of the Table 3 gives results obtained with a direct (forward) numerical solution using soil hydraulic parameters fitted to independently measured hydraulic data obtained with the evaporation method, the steady state unsaturated vertical flow measurements, and the pressure chamber.

Notice that only θ_s was optimized when the objective function was defined in terms of cumulative infiltration data and the tensiometer readings. Optimizations can lead to unrealistic values of the optimized parameters θ_r and/or θ_s when no information about the water content is included in the objective function and the initial condition is given in terms of the pressure head. Only the water content range can then be op-

Table 3. Summary of Parameter Estimation Results for Experiment III

Objective Function	$\Phi(I, \theta_f; \theta_r, \theta_s, \alpha_w, n, K_s)$	$\Phi(I, \theta; \theta_r, \theta_s, \alpha_w, n, K_s)$	$\Phi(I, h; \theta_s, \alpha_w, n, K_s)$	$\Phi(I, h, \theta; \theta_r, \theta_s, \alpha_w, n, K_s)$	$\Phi(I, h, \theta; \theta_r, \theta_s, \alpha_w, n, K_s, \alpha_d)$	$\Phi(I, h, \theta; \theta_r, \theta_s, \alpha_w, n, K_s, \alpha_d, l)$	Direct Solution
Φ	0.00526	0.185	0.152	0.390	0.379	0.303[a]	3.858
Φ_I^*	0.00502	0.0175	0.0058	0.0046	0.0048	0.0046[a]	0.557
Φ_h^*	...	...	0.146[a]	0.195	0.184	0.152	0.604
Φ_θ^*	0.000240	0.167	...	0.191	0.191	0.146[a]	2.697
θ_r	0.000	0.001	0.000[b]	0.015	0.016	0.002	0.0761[b]
θ_s	0.325	0.324	0.246	0.334	0.332	0.310	0.348[b]
α_w, cm^{-1}	0.231	0.206	0.196	0.257	0.263	0.171	...
n	1.46	1.43	2.07	1.44	1.42	1.43	1.46[b]
K_s, cm min^{-1}	1.79	1.42	0.623	1.98	2.11	1.59	0.105[b]
α_d, cm^{-1}	...	...	...	...	0.147	0.111	0.0347[b]
l	0.5[b]	0.5[b]	0.5[b]	0.5[b]	0.5[b]	1.97	0.5[b]
R^2	0.998	0.992	0.953	0.956	0.959	0.966[a]	0.775

[a] Best fit for any particular measurement set and the best fit as characterized by the highest R^2 and the lowest value of the objective function Φ.
[b] Parameters fixed during a particular optimization; α_w and α_d are shape parameters for the wetting and drying cycle, respectively.

timized since the residual and saturated water contents are mutually correlated. For this reason we fixed θ_r equal to zero and optimized only θ_s. Although this approach provided the best overall fit of the tensiometer readings, the optimization resulted in unrealistically low values of θ_s (or the water content interval $\theta_s - \theta_r$). Also, the parameter n differed significantly from those obtained with the other optimizations.

Figure 2 shows measured and calculated (fitted) water contents and cumulative infiltration volumes for the third experiment. The VGM soil hydraulic parameters were optimized using the objective function defined in terms of all three measured variables, i.e., cumulative infiltration volumes, tensiometer measurements, and TDR measurements (Table 3, fifth column). Notice the excellent agreement between measured and calculated values for cumulative infiltration. While more scatter appears in the measured water content values (Figure 2b), the final fit correctly reflects the water content pattern. The predicted water contents reach the final value imposed by each supply tension faster than the measured values, which tend to increase more gradually with time and do not quite reach constant values during the short-duration experiment. This may be partly due to space averaging by the TDR probe as compared to the use of nodal (point) values in the numerical solution. We will discuss this issue later in more detail. Figure 2b shows a small underprediction of the water content for supply tensions of 20, 10, and 5 cm. Notice from Table 3 that the results presented in Figure 2 do not represent the best fit of the measured water contents and that significantly better fits were obtained with other combinations of optimized parameters.

Figure 3 shows measured and calculated pressure heads at eight locations below the disc infiltrometer. Since a few tensiometers were not working correctly during the entire experiment, we used only one tensiometer reading for locations (10, 10), (15, 15), (15, 20), and (15, 30). The differences in pressure head readings at two tensiometers located at the same radial coordinates, for example, for (10, 2.5) and (15, 5), reflect local soil heterogeneity. Almost identical readings were obtained for the duplicate readings at coordinates of (10, 5) and (15, 10). The calculation underpredicted the arrival of the water front at both (10, 2.5) and (10, 5) in the immediate vicinity of the tension disc. Agreement was better at location (10, 10) deeper in the profile, while the agreement was excellent at depths of 10 and 20 cm when r was equal to 15 cm.

We continued the measurements for about 2 more hours after we terminated the infiltration of water. The ensuing redistribution part of the experiment could not be described well with the VGM model that ignored hysteresis (Figure 3, time $>$ 340 min). Figure 4 shows measured and calculated pressure heads at the same eight tensiometer locations when an additional soil hydraulic parameter α_d was included into the optimization (Table 3, sixth column) to account for hysteresis. For the hysteretic case we used the model of *Kool and Parker* [1987], who coupled the VGM model with the simplified scal-

Table 4. Summary of Parameter Estimation Results for Experiment IV

Objective Function	$\Phi(I, \theta_f; \theta_r, \theta_s, \alpha_w, n, K_s)$	$\Phi(I, \theta; \theta_r, \theta_s, \alpha_w, n, K_s)$	$\Phi(I, h; \theta_s, \alpha_w, n, K_s)$	$\Phi(I, h, \theta; \theta_r, \theta_s, \alpha_w, n, K_s)$	$\Phi(I, h, \theta; \theta_r, \theta_s, \alpha_w, n, K_s, \alpha_d)$	$\Phi(I, h, \theta; \theta_r, \theta_s, \alpha_w, n, K_s, \alpha_d, l)$	Direct Solution
Φ	0.0131	0.107	0.244	0.424	0.348	0.339[a]	30.18
Φ_I^*	0.0130	0.0241	0.00034[a]	0.0908	0.0466	0.0372	25.42
Φ_h^*	...	...	0.243[a]	0.272	0.252	0.252	0.70
Φ_θ^*	0.0001	0.0830	...	0.0609	0.0495	0.0490[a]	4.06
θ_r	0.105	0.127	0.000[b]	0.001	0.017	0.025	0.0761[b]
θ_s	0.302	0.307	0.470	0.306	0.332	0.332	0.348[b]
α_w, cm^{-1}	0.201	0.219	0.854	0.134	0.197	0.228	...
n	1.56	1.44	1.22	1.30	1.30	1.28	1.46[b]
K_s, cm min^{-1}	1.01	1.08	34.4	0.463	0.764	1.13	0.105[b]
α_d, cm^{-1}	...	...	...	...	0.129	0.150	0.0347[b]
l	0.5[b]	0.5[b]	0.5[b]	0.5[b]	0.5[b]	0.106	0.5[b]
R^2	0.995	0.991	0.991	0.961	0.975	0.979[a]	0.901

[a] Best fit for any particular measurement set.
[b] Parameters fixed during a particular optimization; α_w and α_d are shape parameters for the wetting and drying cycle, respectively.

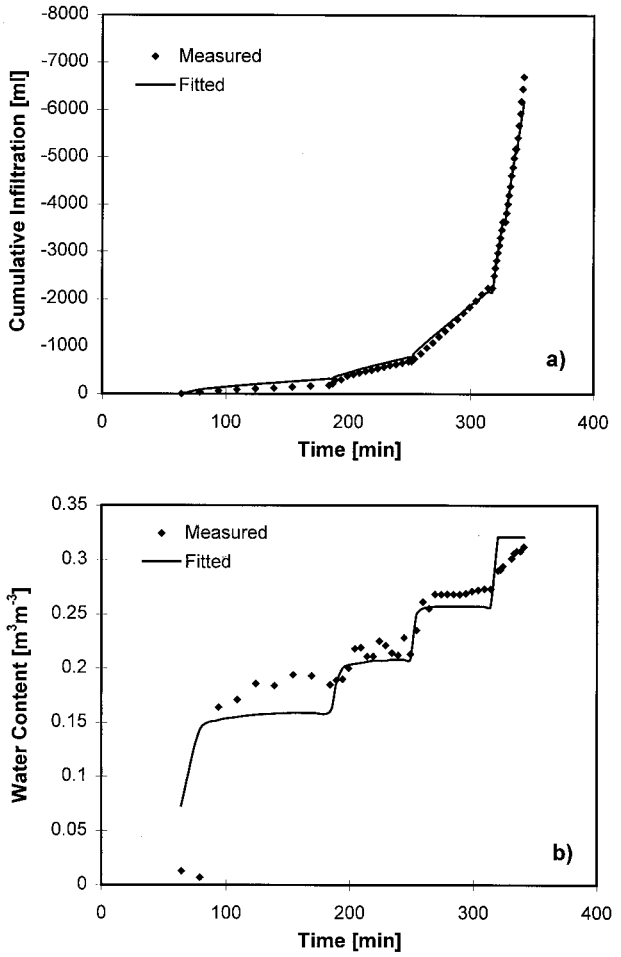

Figure 2. Measured and fitted (a) cumulative infiltration volumes and (b) water contents for the short-duration experiment III. Fitted curves were obtained using optimized van Genuchten-Mualem (VGM) parameters (see Table 3, fifth column).

ing approached of *Scott et al*. [1983] to describe the scanning curves. *Scott et al*. [1983] assumed that the shape parameters for all drying scanning curves are the same as those for the main drying curve and, similarly, the shape parameters for all wetting scanning curves are the same as those for the main wetting curve. Scanning curves are then calculated by varying the residual and saturated water contents for the wetting and drying scanning curves, respectively. *Kool and Parker* [1987] also assumed that the shape parameter n is the same for both wetting and drying, thus decreasing the number of required parameters. Using the additional restrictions that θ_r and θ_s are the same for both drying and wetting, the shape parameter α_d for the drying retention curve (α_w is used for wetting) is the only additional parameter describing hysteresis. An advantage of the model by *Scott et al*. [1983] is that one can obtain the shape parameters of the drying and wetting curves from knowledge of any two main or primary, secondary, or higher-order scanning drying and wetting curves. While the infiltration part of the experiment in Figure 4 is similar to that in Figure 3, a significantly better description of the redistribution part of the experiment is obtained with the simple VGM-H hysteresis approach. The optimized soil hydraulic parameters are very similar to those for Figure 3 (see Table 3). Interestingly, the optimized value of α_d (0.147 cm^{-1}) is close to $\alpha_w/2$ (= 0.132 cm^{-1}), an approximation often thought to be reasonable for simlating hysteresis [*Kool and Parker*, 1987; *Luckner et al*., 1989].

Overall, all optimizations that included in the objective function either water content data or only the initial and final values of the water content at a depth of 2 cm provided similar sets of optimized parameters. The use of pressure head data did not significantly improve the results. The main benefit of using pressure head measurements is the obtaining of information about both infiltration and redistribution and, consequently, about hysteresis in the soil hydraulic properties.

4.2.2. Experiment IV. Parameter estimation results for experiment IV, the 6 day slow infiltration experiment for which steady state was reached for each supply pressure head, are summarized in Table 4. The best fit of cumulative infiltration and pressure head readings was obtained when the objective function did not include water content measurements. The predicted and measured cumulative infiltration volumes were essentially identical (figure not shown). Nevertheless, the estimated soil hydraulic parameters for this optimization were, as for experiment III, unrealistic, producing a high saturated water content and very high values of α and K_s (Table 4). These results suggest that the optimization requires some additional information about the water content. Additional information is usually available for transient laboratory experiments (such as outflow or evaporation experiments) in terms of the total water volume in the sample but generally not for field experiments. For example, *Inoue et al*. [1998] analyzed a multistep soil water extraction field experiment and obtained unrealistically high estimates of the residual water content (θ_s was fixed) when using only pressure head data and cumulative extraction rates despite having an excellent fit of these data. Estimation of the retention curve dramatically improved only when water content data were included in the optimization [see *Inoue et al*., 1998, Figure 10]. Similarly, estimates of θ_s (θ_r was fixed) were very unreliable when only pressure head and cumulative infiltration data were analyzed in a modified cone penetrometer experiment [*Kodešová et al*., 1998; *Šimůnek et al*., 1999]. Fixing θ_s or including water content data in the latter example improved the estimation. Consistent with these results, *Šimůnek and van Genuchten* [1997] found out that the identifiability of soil hydraulic parameters from numerically generated disc infiltrometer data dramatically improved when the initial condition was expressed in terms of the water content instead of the pressure head.

Figure 5 shows measured and calculated water contents and cumulative infiltration rates for the overall best fit, i.e., when the objective function was defined in terms of all measured variables (Table 4, seventh column). Some interruptions occurred in the collection of cumulative infiltration and water content data during the nights; however, tensiometer readings continued since they were logged in automatically. The water content again gradually increased with time for each supply pressure head during the entire experiment and did not reach a constant value. The water content increased long after the numerical model reached a constant water content and in spite of the infiltration rates being already constant. Again, as for the third example, this could be caused by water content averaging over a relatively large volume when using the TDR probe, while the numerical solution only assumed nodal values. An equally or more probable explanation is that water moves only gradually into relatively small intra-aggregate or dead-end pores that do not significantly contribute to water flow. Water initially may move primarily through the larger pores (depend-

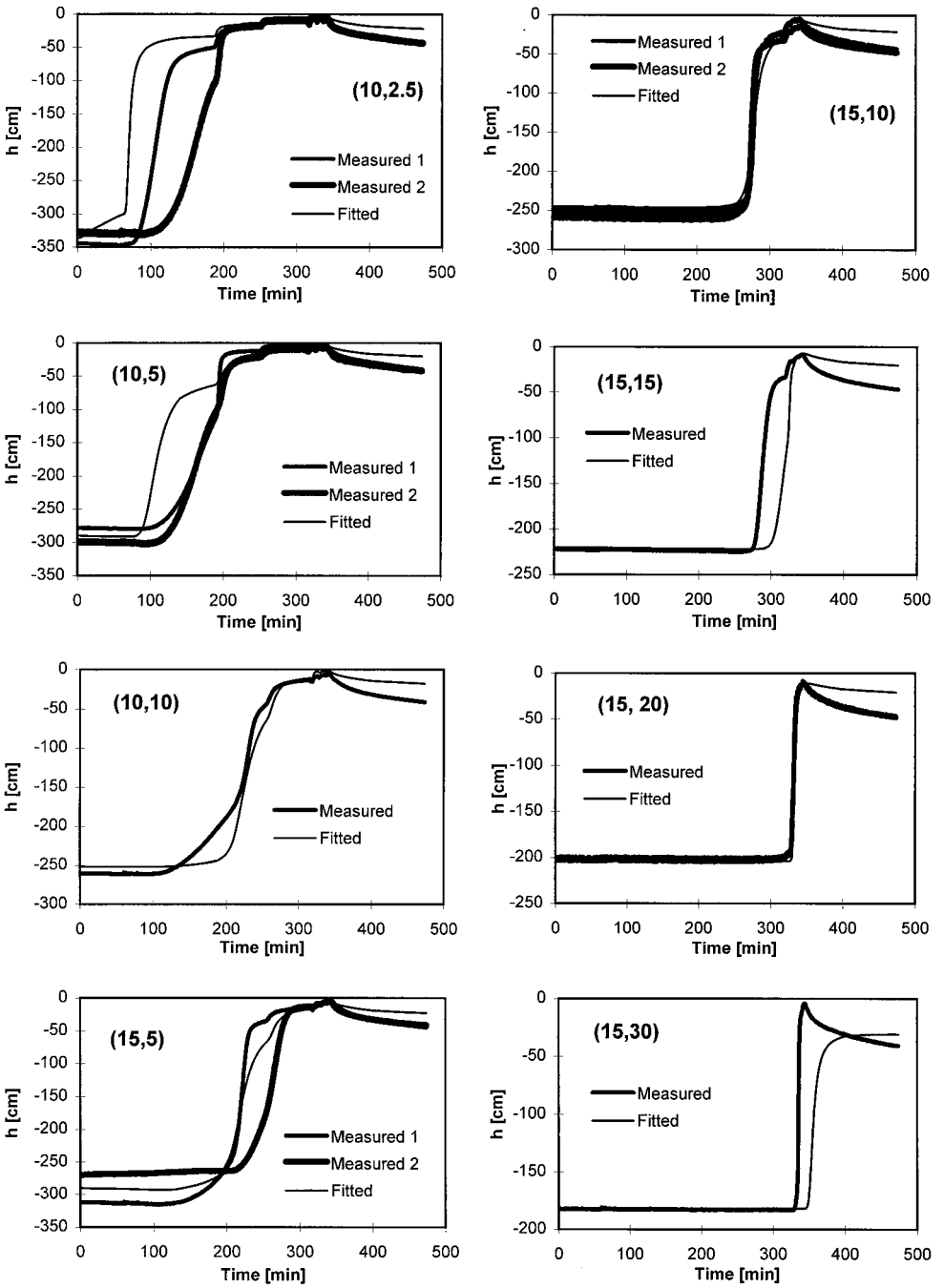

Figure 3. Measured and fitted pressure heads at eight locations below the disc infiltrometer for the short-duration experiment III. Calculated curves were obtained using optimized VGM parameters (see Table 3, fifth column).

ing upon the supply tension) that provide the main paths for water flow. These larger pores are the most important in terms of defining the overall flow process and determining the tensiometer pressure heads; water hence may bypass the smaller pores, which are vulnerable to air entrapment. This situation would cause the pressure head and the infiltration rates to reach apparent steady state conditions much faster than the water content. Notice from Figure 6 that the measured pressure heads indeed reached equilibrium conditions faster than the numerically calculated pressure heads. A similar water flow nonequilibrium situation was observed by *Wang et al*. [1998], who measured increases in the water content under the tension infiltrometer long after tensiometers had reached equilibrium at the same spatial coordinates. While the agreement between measured and fitted cumulative volumes in Figure 5 was worse than the best fit mentioned above, the match was still relatively good. For the optimized parameters the numerical code overpredicted and underpredicted the infiltration rates for supply tensions of 10 and 1 cm, respectively.

Figure 6 shows again the measured and calculated pressure heads at eight tensiometer locations. Inserts give details about the pressure head at early times. Notice again an underpredic-

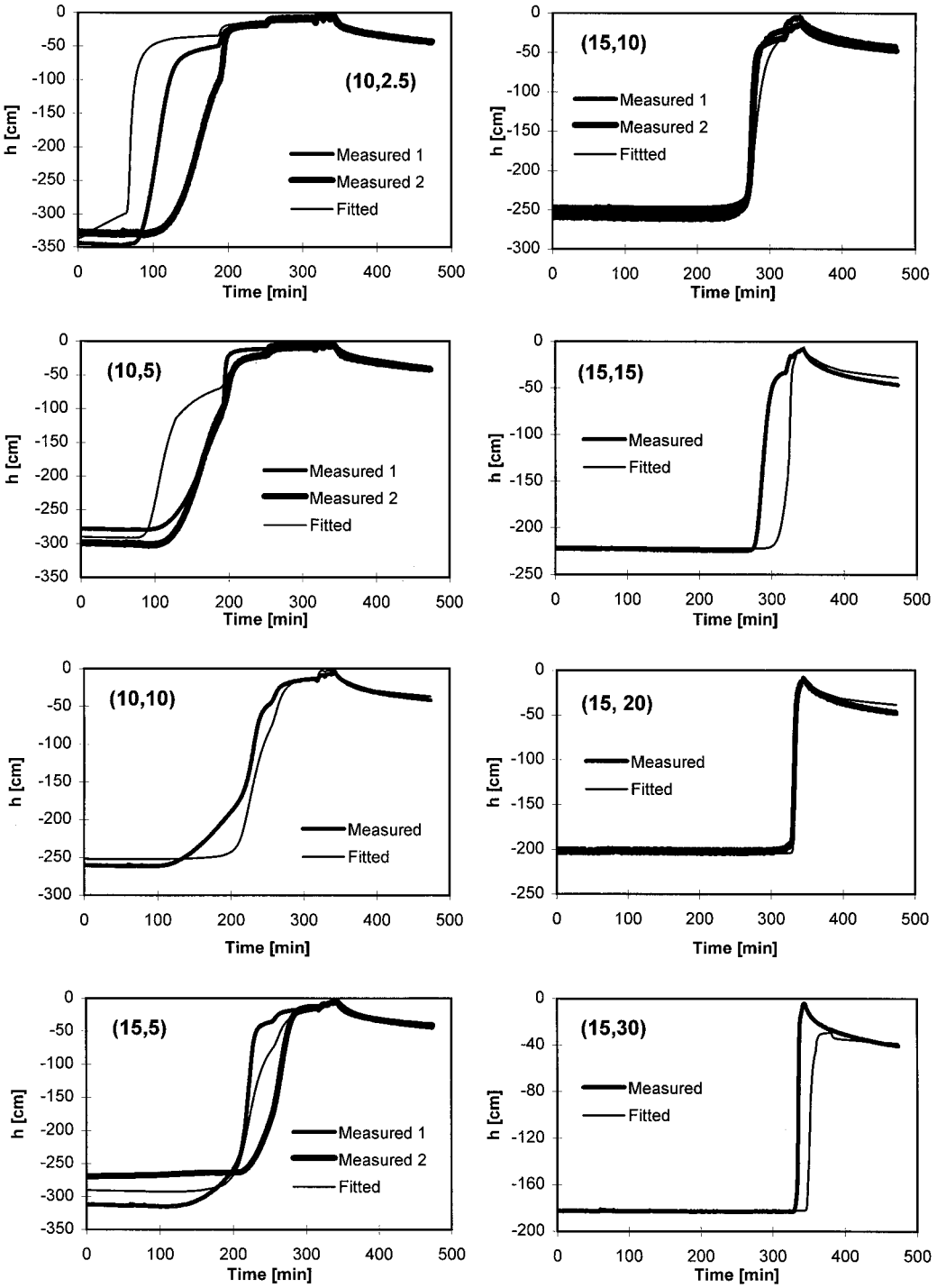

Figure 4. Measured and fitted pressure heads at eight locations below the disc infiltrometer for the short-duration experiment III. Calculated curves were obtained using optimized VGM parameters with hysteresis (VGM-H) (see Table 3, sixth column).

tion of the moisture front arrival at a depth of 2.5 cm and a relatively good agreement at other locations having a radial coordinate of 10 cm. There is an especially good correspondence between the measured and calculated pressure heads for locations with a radial coordinate of 15 cm at depths of 5 and 10 cm, whereas the model predicts later arrivals of the moisture front to depths of 20 and 30 cm. Once again, all optimizations that included in the objective function either water content measurements or only the initial and final values of water content at a depth of 2 cm provided similar sets of optimized parameters.

4.3. Measured and Optimized Soil Hydraulic Properties

Soil water retention data determined with the evaporation method for $h > -700$ cm and in a pressure chamber for $h = -10$ and -150 m for 10 samples are presented in Figure 7a. Corresponding hydraulic conductivities estimated using the evaporation method for $h < -10$ cm and those obtained using

the tension disk infiltrometer for $h = -1$, -5, and -10 cm are shown in Figure 7b. Overall, the results obtained for all 10 samples using the evaporation method show a high level of consistency. Also, the $K(h)$ relations in the wet range estimated from the infiltration experiments correspond reasonably well with those in the drier range determined using the evaporation method. The soil hydraulic parameters were obtained by simultaneously fitting (6) and (7) to all $\theta(h)$ and $K(h)$ data using the retention curve (RETC) code [*van Genuchten et al.*, 1991]. We obtained an excellent fit when the parameter l was fixed at 0.5 for the evaporation data (Figure 7, fit 1). The fit, however, overpredicted water contents at the higher tensions and underpredicted the hydraulic conductivity at a pressure head of -1 cm. A summary of the obtained soil hydraulic parameters, together with R^2, is given in Table 5. A better description of the retention curve at higher tensions was obtained when the parameter l was also considered to be an unknown. Since the first fit provided a better description of the soil hydraulic data within the experimental range for our laboratory tension disc experiments, we used these parameters for the direct solutions given in Tables 3 and 4.

Figure 8 shows retention curves obtained with the parameter estimation method for experiments III and IV and, for comparison purposes, results produced with the evaporation method. Even though different optimization options were used, the resulting retention curves for each experiment are very similar; they define a relatively narrow band and converge to approximately the same saturated water content. Notice that we plotted both the wetting and drying curves when hysteresis was considered. The retention curves estimated from experiment IV gave higher water contents over nearly the entire h range than those estimated from experiment III. The greatest difference between the two tests is ~0.04 and occurs at a pressure head of ~-100 cm. Although all retention curves have similar shapes, the curves obtained by parameter estimation do underestimate water contents at particular pressure heads relative to curves based on the evaporation method. This underestimation is more important for retention curves determined from the short-duration experiment III than for the long-duration experiment IV. The average difference between retention curves determined from experiment IV and the evaporation method is again ~0.04 cm^3 cm^{-3}. This difference can be explained partly by hysteresis, partly by entrapped air, and partly by observed nonequilibrium behavior.

Since the soil samples used for the evaporation method were initially saturated with deionized water, the resulting retention curve represents the main drying curve with θ_s approximately equal to porosity. It is generally accepted that the field-saturated (or satiated) water content is much smaller than porosity because of entrapped air. Part of the difference can also be explained by the presence of flow irregularities and deviations from equilibrium flow theory (such as a gradually increasing water content even when the infiltration rate and the pressure head reached steady state). For both experiments the water content was 0.185 after 2 hours of infiltration. For experiment IV the water content increased another 0.044 units before the end of the tension infiltration step (-20 cm). The water content increased ~0.025 even after tensiometers located at deeper depth than TDR reached a constant value. Since the water content measurements are included in the definition of the objective function, but somehow lag in time behind the pressure heads, the optimization routines must underestimate the water content at particular pressure heads.

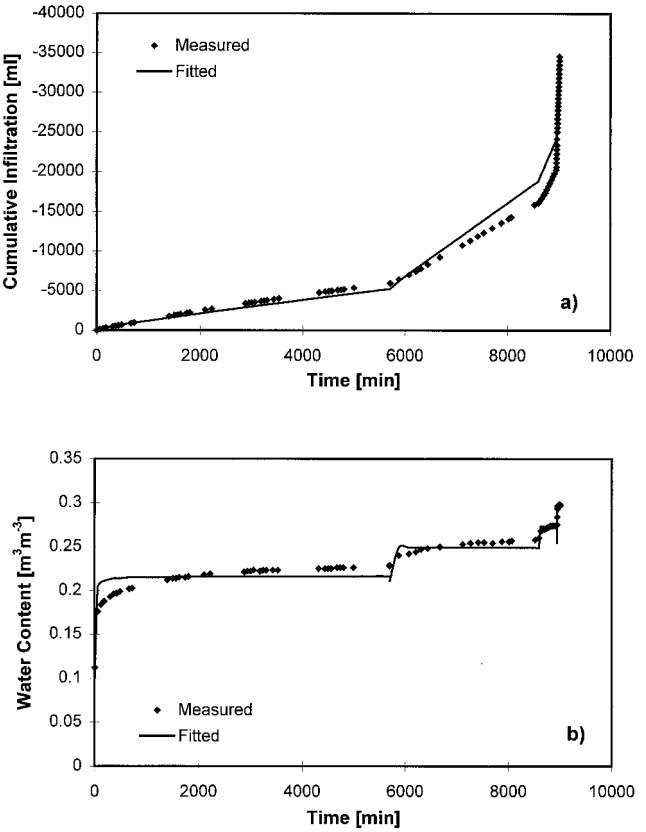

Figure 5. Measured and fitted (a) cumulative infiltration volumes and (b) water contents for the long-duration experiment IV. Calculated curves were obtained using optimized VGM parameters with hysteresis (VGM-Hl) (see Table 4, seventh column).

Figure 9 shows hydraulic conductivities determined directly using the evaporation method, those measured during the steady state infiltration, and estimated conductivity functions assuming different optimization options for experiments III and IV. The optimized hydraulic conductivities fall in the same range as those measured during steady state infiltration and those calculated using *Wooding*'s [1968] analysis. Good correspondence between conductivities obtained using Wooding's approach and the inverse results were expected since both methods analyze the same data. While hydraulic conductivities measured during steady state infiltration correspond closely with the $K(h)$ functions estimated from experiment IV, Wooding's conductivities are closer to the results from experiment III. The hydraulic conductivities estimated from experiment III were higher than those estimated from experiment IV at the lower tensions and tended to converge toward higher tensions. The average K_s estimated from experiments III and IV were ~1.75 and 0.9 cm min^{-1}, respectively. The evaporation method provided slightly higher values of the conductivities at particular tensions than those estimated by numerical inversion. Nevertheless, the drying branches of the hydraulic conductivity functions are very close to point values obtained with the evaporation method.

5. Concluding Remarks

The parameter estimation technique proved to be a powerful method for analyzing transient water flow experiments.

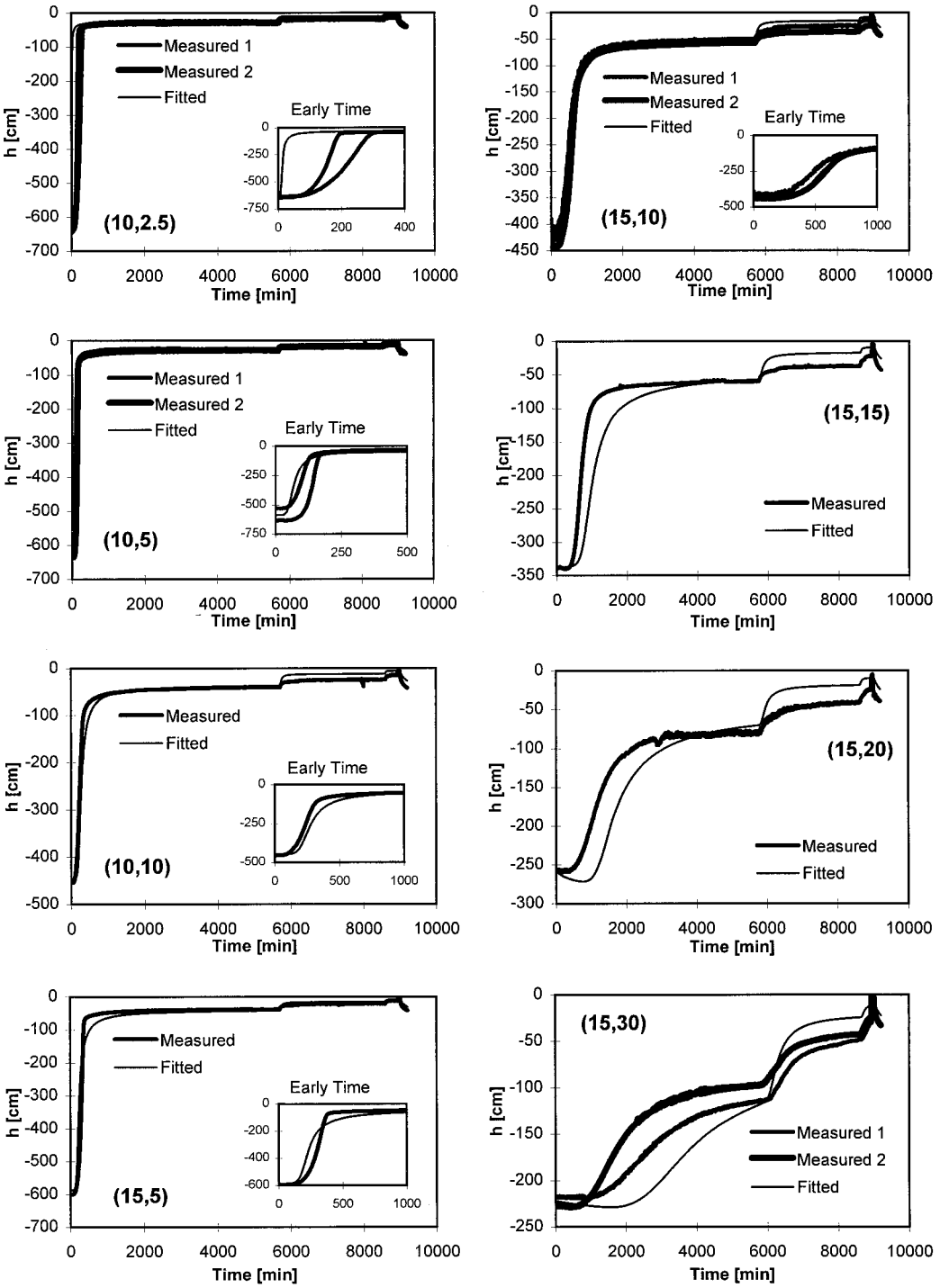

Figure 6. Measured and fitted pressure heads at eight locations below the disc infiltrometer for the long-duration experiment IV. Calculated curves were obtained using optimized VGM parameters with hysteresis (VGM-Hl) (see Table 4, seventh column). Inserts give details of pressure heads at the early time.

Unsaturated hydraulic conductivities obtained with parameter estimation corresponded well with results of *Wooding*'s [1968] analysis as well as with those determined with steady state infiltration. Drying branches of the $K(h)$ function determined by parameter estimation corresponded relatively well with hydraulic conductivities obtained by the evaporation method. Retention curves estimated from the infiltration experiments were quite different from those determined using the evaporation method. They, nevertheless, may prove to be more useful in describing infiltration and the transport of contaminants through the vadose zone than retention curves determined by steady state methods or from transient processes of a totally different nature.

An advantage of axisymmetric experiments, such as those discussed in this paper, is that one can have several measurements at locations with the same radial coordinates. However,

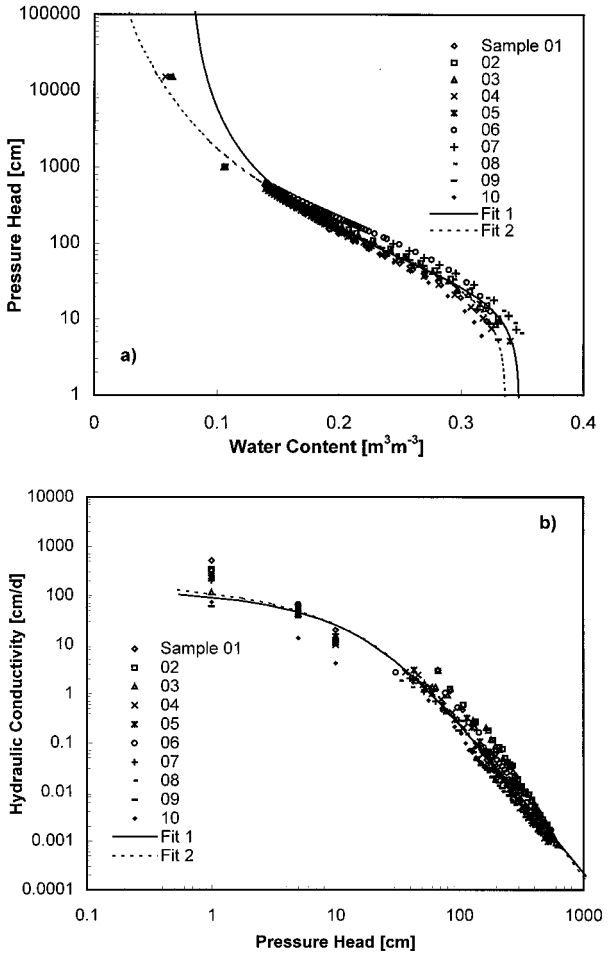

Figure 7. (a) Soil water retention curves determined with the evaporation method for $h > -700$ cm and as determined with a pressure chamber for $h = -10$ and -150 m and (b) hydraulic conductivity functions determined with the evaporation method for $h < -10$ cm and using a tension infiltration method for $h = -1$, -5, and -10 cm.

these measurements do not necessarily provide the same results because of local soil heterogeneity. Figure 10 shows idealized but typical tensiometer responses of such duplicate measurements in the soil profile with each tensiometer showing a relatively sharp curve. An interesting question is how best to analyze these curves when they differ significantly. If the response curves were analyzed independently, the sharp wetting

Table 5. Soil Hydraulic Parameters Fitted to the Combined Data Measured With the Evaporation Method, the Pressure Chamber, and the Steady State Tension Infiltration

Parameter	Fit 1	Fit 2
θ_r	0.0761	0
θ_s	0.348	0.337
α_d, cm^{-1}	0.0347	0.0303
n	1.46	1.31
K_s, cm d^{-1}	151.4	255.1
l	0.5[a]	2.23
R^2	0.967	0.968

[a] Parameter fixed during optimization.

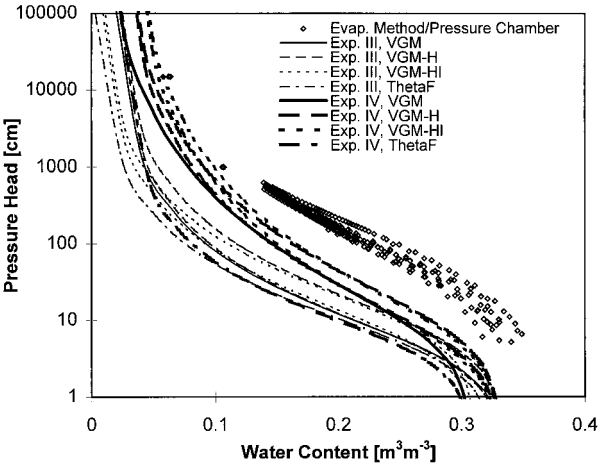

Figure 8. Soil water retention curves determined using different optimization options and data collected for experiments III and IV. Retention data were measured using the evaporation method and the pressure chamber.

fronts for both cases would probably result in fairly similar optimized shape parameters (α, n), while the optimized value of K_s could be quite different between the two optimizations. The arithmetic or geometric mean of these two values could then be taken as the effective hydraulic conductivity of the soil. One could also use mean value of the measured variable, or one could define the objective function in terms of both measurements, in which case the optimization probably will result in the same mean hydraulic conductivity but with widely different optimized shape parameters α and n. The optimized parameters will then predict a much more gradual moisture front as shown by the dotted line in Figure 10. Such a wetting front would be characteristic of a more fine-textured soil (especially a lower n value). This tendency toward predicting soil hydraulic parameters of finer soils is a general trend caused by this type of averaging of measured pressure heads. A more appropriate way of averaging measured variables at the same

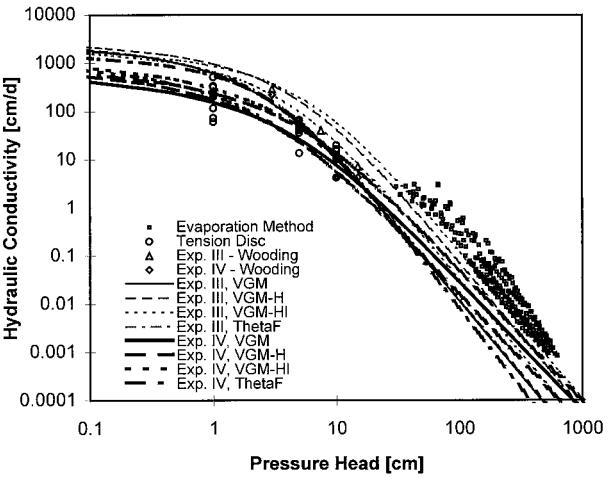

Figure 9. Hydraulic conductivity functions determined using different optimization options and data collected for experiments III and IV. Hydraulic conductivities were measured using the evaporation method and making use of *Wooding*'s [1968] analysis of tension disc experiments III and IV as well as steady state infiltration experiments.

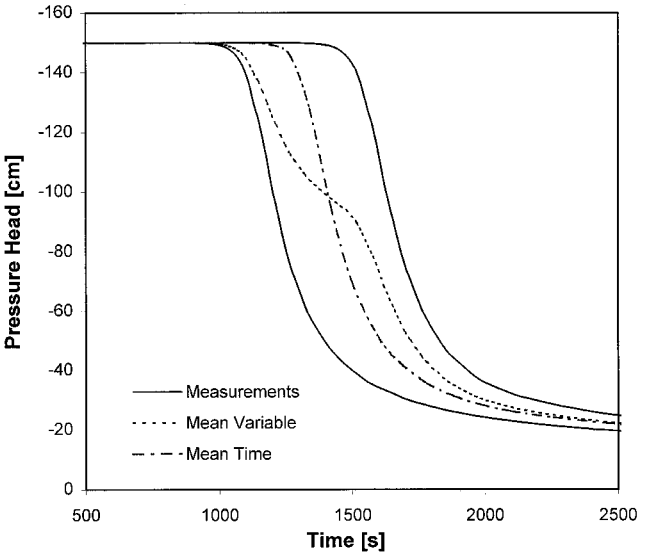

Figure 10. Hypothetical pressure head profiles at a nodal point with coordinates (r, z) and possible averaging at given values of time or the pressure head.

radial coordinates seems to be to use the mean time for the same value of the measured variable (dash-dotted line in Fig. 10) rather than the mean for the same time. This alternative type of averaging would lead to the correct shape parameters (α, n) and to approximately the correct (mean) K_s.

Acknowledgment. Thanks are due to N. Romano for his many useful review suggestions and comments.

References

Ankeny, M. D., M. Ahmed, T. C. Kaspar, and R. Horton, Simple field method for determining unsaturated hydraulic conductivity, *Soil Sci. Soc. Am. J.*, *55*, 467–470, 1991.

Bouma, J., D. I. Hillel, F. D. Hole, and C. R. Amerman, Field measurement of unsaturated hydraulic conductivity of unsaturated soil near saturation, *Soil Sci. Soc. Am. Proc.*, *35*, 362–364, 1971.

Císlerová, M., J. Šimůnek, and T. Vogel, Changes of steady-state infiltration rates in recurrent ponding infiltration experiments, *J. Hydrol.*, *104*, 1–16, 1988.

Clothier, B. E., M. B. Kirkham, and J. E. McLean, In situ measurement of the effective transport volume for solute moving through soil, *Soil Sci. Soc. Am. J.*, *56*, 733–736, 1992.

Cuenca, R. H., et al., Soil measurements during HAPEX-Sahel intensive observation period, *J. Hydrol.*, *188-189*, 224–266, 1997.

Gardner, W. R., Some steady-state solutions of the unsaturated moisture flow equation with application to evaporation from a water table, *Soil Sci.*, *85*, 228–232, 1958.

Hollenbeck, K. J., and K. H. Jensen, Experimental evidence of randomness and nonuniqueness in unsaturated outflow experiments designed for hydraulic parameter estimation, *Water Resour. Res.*, *34*, 595–602, 1998.

Inoue, M., J. Šimůnek, J. W. Hopmans, and V. Clausnitzer, In-situ estimation of soil hydraulic functions using a multi-step soil water extraction technique, *Water Resour. Res.*, *34*, 1035–1050, 1998.

Jarvis, N. J., and I. Messing, Near-saturated hydraulic conductivity in soils of contrasting texture measured by tension infiltrometers, *Soil Sci. Soc. Am. J.*, *59*, 27–34, 1995.

Kachanoski, R. G., I. J. Van Wesenbeeck, P. Von Bertoldi, A. Ward, and C. Hamplen, Measurement of soil water content during three-dimensional axial-symmetric water flow, *Soil Sci. Soc. Am. J.*, *54*, 645–649, 1990.

Kodešová, R., M. M. Gribb, and J. Šimůnek, Estimating soil hydraulic properties from transient cone penetrometer data, *Soil Sci.*, *163*, 436–453, 1998.

Kool, J. B., and J. C. Parker, Development and evaluation of closed-form expressions for hysteretic soil hydraulic properties, *Water Resour. Res.*, *23*, 105–114, 1987.

Logsdon, S. D., E. L. McCoy, R. R. Allmaras, and D. R. Linden, Macropore characterization by indirect methods, *Soil Sci.*, *155*, 316–324, 1993.

Luckner, L., M. T. van Genuchten, and D. R. Nielsen, A consistent set of parametric models for the two-phase flow of immiscible fluids in the subsurface, *Water Resour. Res.*, *25*, 2187–2193, 1989.

Marquardt, D. W., An algorithm for least-squares estimation of nonlinear parameters, *SIAM J. Appl. Math.*, *11*, 431–441, 1963.

Mualem, Y., A new model for predicting the hydraulic conductivity of unsaturated porous media, *Water Resour. Res.*, *12*, 513–522, 1976.

Perroux, K. M., and I. White, Design for disc permeameters, *Soil Sci. Soc. Am. J.*, *52*, 1205–1215, 1988.

Quadri, M. B., B. E. Clothier, R. Angulo-Jaramillo, M. Vauclin, and S. R. Green, Axisymmetric transport of water and solute underneath a disk permeameter: Experiments and numerical model, *Soil Sci. Soc. Am. J.*, *58*, 696–703, 1994.

Reynolds, W. D., and D. E. Elrick, Determination of hydraulic conductivity using a tension infiltrometer, *Soil Sci. Soc. Am. J.*, *55*, 633–639, 1991.

Russo, D., E. Bresler, U. Shani, and J. C. Parker, Analysis of infiltration events in relation to determining soil hydraulic properties by inverse problem methodology, *Water Resour. Res.*, *27*, 1361–1373, 1991.

Scott, P. S., G. J. Farquhar, and N. Kouwen, Hysteresis effects on net infiltration, in *Advances in Infiltration*, *Publ. 11-83*, pp. 163–170, Am. Soc. of Agric. Eng., St. Joseph, Mich., 1983.

Šimůnek, J., and M. T. van Genuchten, Estimating unsaturated soil hydraulic properties from tension disc infiltrometer data by numerical inversion, *Water Resour. Res.*, *32*, 2683–2696, 1996.

Šimůnek, J., and M. T. van Genuchten, Estimating unsaturated soil hydraulic properties from multiple tension disc infiltrometer data, *Soil Sci.*, *162*, 383–398, 1997.

Šimůnek, J., M. Šejna, and M. T. van Genuchten, The HYDRUS-2D software package for simulating water flow and solute transport in two-dimensional variably saturated media: Version 1.0, *IGWMC-TPS-53*, 167 pp., Int. Ground Water Model. Cent., Colo. Sch. of Mines, Golden, 1996.

Šimůnek, J., R. Angulo-Jaramillo, M. G. Schaap, J.-P. Vandervaere, and M. T. van Genuchten, Using an inverse method to estimate the hydraulic properties of crusted soils from tension disc infiltrometer data, *Geoderma*, *86*, 61–81, 1998a.

Šimůnek, J., O. Wendroth, and M. T. van Genuchten, A parameter estimation analysis of the evaporation method for determining soil hydraulic properties, *Soil Sci. Soc. Am. J.*, *62*, 894–905, 1998b.

Šimůnek, J., R. Kodešová, M. M. Gribb, and M. T. van Genuchten, Estimating hysteresis in the soil water retention function from modified cone penetrometer test, *Water Resour. Res.*, *35*, 1329–1345, 1999.

Smettem, K. R. J., and B. E. Clothier, Measuring unsaturated sorptivity and hydraulic conductivity using multiple disk permeameters, *J. Soil Sci.*, *40*, 563–568, 1989.

van Genuchten, M. T., A closed-form equation for predicting the hydraulic conductivity of unsaturated soils, *Soil Sci. Soc. Am. J.*, *44*, 892–898, 1980.

van Genuchten, M. T., F. J. Leij, and S. R. Yates, The RETC code for quantifying the hydraulic functions of unsaturated soils, *EPA/600/2-91-065*, Off. of Res. and Dev., U.S. Environ. Prot. Agency, Washington, D. C., 1991.

van Genuchten, M. T., F. J. Leij, and L. Wu (Eds.), *Characterization and Measurement of the Hydraulic Properties of Unsaturated Porous Media*, Univ. of Calif., Riverside, Calif., 1999.

Vogeler, I., B. E. Clothier, S. R. Green, D. R. Scotter, and R. W. Tillman, Characterizing water and solute movement by time domain reflectometry and disk permeametry, *Soil Sci. Soc. Am. J.*, *60*, 5–12, 1996.

Wang, D., S. R. Yates, and F. F. Ernst, Determining soil hydraulic properties using tension infiltrometers, time domain reflectometry, and tensiometers, *Soil Sci. Soc. Am. J.*, *62*, 318–325, 1998.

Ward, A. L., R. G. Kachanoski, and D. L. Elrick, Laboratory measurements of solute transport using time domain reflectometry, *Soil Sci. Soc. Am. J.*, *58*, 1031–1039, 1994.

Wendroth, O., and J. Šimůnek, Soil hydraulic properties determined from evaporation and tension infiltration experiments and their use

for modeling field moisture status, in *Characterization and Measurement of the Hydraulic Properties of Unsaturated Porous Media*, edited by M. T. van Genuchten, F. J. Leij, and L. Wu, pp. 737–748, Univ. of Calif., Riverside, Calif., 1999.

Wendroth, O., W. Ehlers, J. W. Hopmans, H. Kage, J. Halbertsma, and J. H. M. Wösten, Reevaluation of the evaporation method for determining hydraulic functions in unsaturated soils, *Soil Sci. Soc. Am. J.*, *57*, 1436–1443, 1993.

White, I., and M. J. Sully, Macroscopic and microscopic capillary length and time scales from field infiltration, *Water Resour. Res.*, *23*, 1514–1522, 1987.

Wind, G. P., Capillary conductivity data estimated by a simple method, in *Water in the Unsaturated Zone*, edited by P. E. Rijtema and H. Wassink, vol. 1, pp. 181–191, Int. Assoc. of Sci. Hydrol., Gentbrugge, Germany, 1968.

Wooding, R. A., Steady infiltration from large shallow circular pond, *Water Resour. Res.*, *4*, 1259–1273, 1968.

J. Šimůnek and M. T. van Genuchten, U. S. Salinity Laboratory, USDA-ARS, 450 West Big Springs Road, Riverside, CA 92507. (JSimunek@ussl.ars.usda.gov)

O. Wendroth, Institute for Soil Landscape Research, ZALF, Eberswalder Straße 84, D-15374 Müncheberg, Germany.

(Received October 9, 1998; revised May 10, 1999;
accepted June 1, 1999.)